

90-Mev Neutron-Proton Scattering at Large Proton Angles*

ROGER WALLACE

Radiation Laboratory, Department of Physics, University of California, Berkeley, California

(Received October 13, 1950)

Neutron-proton scattering with 90-Mev neutrons has been investigated by others, using a proportional counter technique and also using a cloud chamber, and the scattering cross section for neutrons for center-of-mass angles from 36° to 180° has been measured. The present experiment was an attempt to overlap the data of Hadley, *et al.*, from 74° to 36° and to extend the cross-section measurements to smaller angles. This experiment was performed with nuclear emulsions in order to permit the detection of protons down to about 1.5 Mev, and to avoid systematic errors which might be present in the case of other methods of detection. The results agree with those of Hadley, *et al.*, within the probable error, and the cross-section curve exhibits beyond 36° the same general trend as does their curve.

I. INTRODUCTION

NEUTRON-PROTON scattering cross sections have been measured by several different investigators, using the 90-Mev neutrons from the 184-in. Berkeley cyclotron. Hadley, *et al.*,¹ used two different arrangements of proportional counters. Their points do not lie on a curve that is symmetrical about 90° . The present experiment was performed to find whether the cross section rises in the small angle region. It has been felt by some that the cross-section curve was perhaps flat beyond 70° and did not rise. The results of this experiment serve to confirm the rising slope of the curve in the small angle range, in agreement with Hadley *et al.* Brueckner, *et al.*,² using a cloud-chamber technique, have observed an angular dependence of the $n-p$ cross section similar to that observed by Hadley and his co-workers. The results of the present experiment also agree well with the cloud-chamber data.

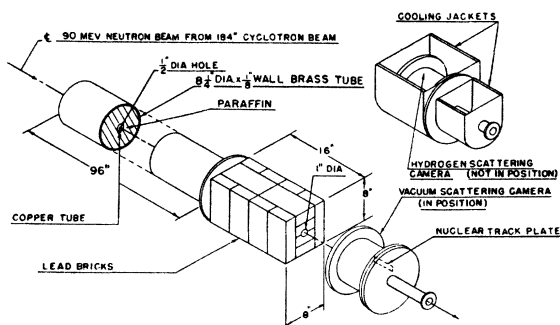


FIG. 1. Arrangement of the paraffin collimator and lead bricks in front of the scattering camera. The alternate cameras are shown. The vacuum camera is shown in bombardment position. The jacketed hydrogen chamber is shown at one side. The wood supports for the apparatus are not shown. Twelve nuclear track plates were arranged symmetrically around the beam at 30° intervals, of which one is indicated in the figure.

* This paper is based on work performed under the auspices of the AEC.

¹ Hadley, Kelly, Leith, Segrè, Wiegand, and York, *Phys. Rev.* **75**, 351 (1949).

² Brueckner, Hartsough, Hayward, and Powell, *Phys. Rev.* **75**, 555 (1949).

II. APPARATUS AND PROCEDURE

The main part of the apparatus consisted of a nuclear plate camera, similar in design to that used by Panofsky and Fillmore.³ The camera and associated shielding (Fig. 1) were mounted on a support, aligned in the 90-Mev neutron beam of the 184-in. cyclotron, similar to the paraffin collimator mount used by Brueckner, *et al.*² The collimator was stopped down to a $\frac{1}{2}$ -in. diameter circle and additional lead bricks were added to reduce the background. The camera (Fig. 2) differed from that used by Panofsky and Fillmore³ in that the plates were mounted farther from the beam and farther from each other. These dimensional changes were made since the neutron beam intensity of the cyclotron is much less than the proton beam intensity of the linear accelerator; thus it was necessary to include more beam area with a consequent relaxation of the geometrical precision of the experiment. At each end of the camera-scattering chamber there was a 0.005-in. duraluminum foil window. The cyclotron beam, collimated to $\frac{1}{2}$ in. passed into and out of the camera through these foils. The exit foil was mounted on the end of a tube, as

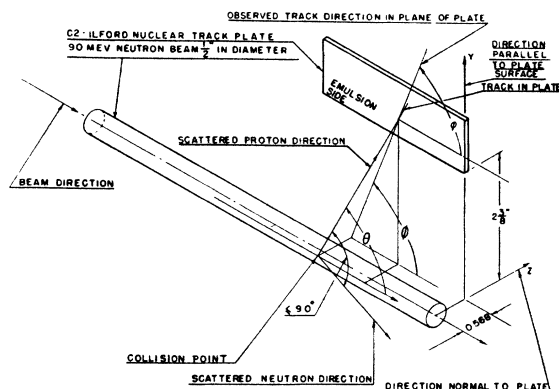


FIG. 2. Geometrical location of the nuclear track plates relative to the neutron beam. The variables used in the measurements and calculations are shown. All variables are in the laboratory system. The relations between the scattering angle θ and the observed angle ϕ are indicated.

³ W. K. H. Panofsky and F. L. Fillmore, *Phys. Rev.* **79** 57 (1950).

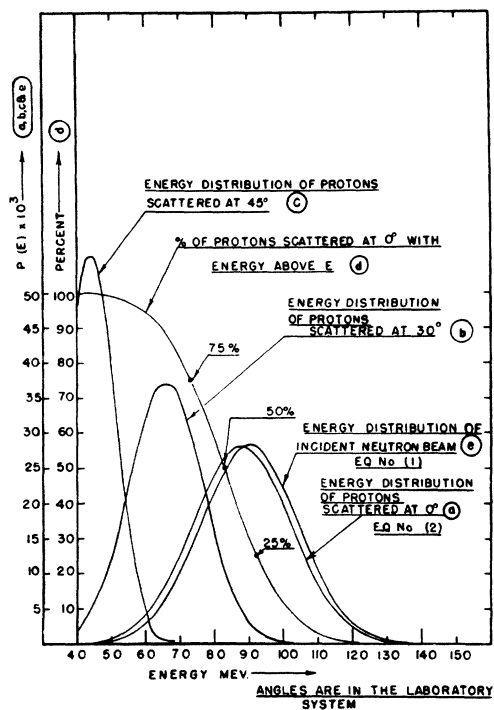


FIG. 3. Functions dependent on the energy. Curves (a), (b), and (c) are the probability of a recoil proton being scattered at 0° , 30° , or 45° having a particular energy. It is seen that the absolute dispersion in energy decreases as the scattering angle increases. Curve (d) gives the percentage of the protons scattered at 0° with energy above a definite value E . This curve is secured directly from curve (e), the energy distribution of the "90-Mev" neutron beam from the 184-in. Berkeley cyclotron.

shown in Fig. 2, in order to reduce the background, on the plates, that might have come from particles scattered from the exit foil. Particles which might have been scattered from the entrance foil entered the plates at such an angle that tracks caused by them, when viewed under a microscope, were easily distinguished from those coming from the hydrogen gas contained in the scattering chamber, since the desired tracks and the foil scattered tracks entered the field of view from different angular directions. Thus the particles scattered from the entrance foil constitute a nonconfusable background.

Four point screw supports permitted the paraffin collimator and the camera to be aligned coaxially within $\frac{1}{16}$ in. The alignment was carried out with an optical telescope and was checked by exposing, during the first few minutes of the cyclotron run, an x-ray film located in a known position on the camera. A $\frac{1}{16}$ -in. alignment tolerance does not introduce a first-order source of error since the plates were arranged symmetrically around the beam and the angular distribution data from all plates were combined. The plates were aligned in the camera by being held against a machined surface for which the geometric tolerance was less than 0.010 in.

Two identical cameras were constructed, one for hydrogen exposures, the other for vacuum-background

exposures. The exposures from which the data were taken were made for 405 min at an average of $27\frac{1}{2}$ R per hour for the hydrogen run, and 65 min at an average of 28 R per hour for the vacuum run. This made the hydrogen run 186 R and the neutron background run 30 R. This intensity (the R-unit is an arbitrary measure of intensity) corresponds to a neutron flux of approximately 10^6 neutrons/cm² sec.

The first few trial runs with hydrogen in the camera resulted in completely blackened plates. At first it was thought that the blackening was caused by impurities in the hydrogen gas, so the hydrogen was passed through a hot palladium leak, thus separating all other elements with the possible exception of a minute trace of helium. Since the blackening still occurred with this purified hydrogen it was concluded that the hydrogen itself must attack the emulsion. Webb⁴ advised us later that it was possible that the photographic emulsions were fogged by pure hydrogen gas. The reason that Panofsky and Fillmore³ did not experience this difficulty was that they used a lower hydrogen pressure than the two atmospheres used in this experiment, and somewhat shorter times during which the plates were exposed to the hydrogen. It was found that the blackening of the plates by the hydrogen was temperature sensitive, and that a reduction of temperature to -15° to -20°C would allow the plates to be only slightly fogged after 8 hours exposure. Consequently, a jacket filled with a eutectic mixture of rock salt and ice was installed, during the run, around the camera intended for hydrogen exposure. The plate temperature was thus maintained at about -15°C . Webb indicated that a reduction of the temperature to -15°C would probably not reduce the proton sensitivity of the plates.

The data were taken from the plates with a microscope, operating at $570\times$, scanning a swath 140 microns wide. The recoil proton tracks were identified by their specific ionization, their point of entrance dive angles into the emulsion, their azimuth angle in the microscope field, and their range. When a track seen to start in the field of the microscope had been recognized as that of a proton by its ionization density, the microscope was focused up and down to check the fact that the track dived into the emulsion at an angle that was compatible with the geometric location of the photographic plate relative to the neutron beam. If the track passed this test, the plate was moved until the point at which the track entered the emulsion was centered under the microscope reticule cross hairs. The cross hairs were then rotated until one was tangent to the track as near to the point of entry as possible. Panofsky and Fillmore³ explain how this can be done with a minimum of setting error. The azimuth angle of the entry point was then measured with a goniometer attached to one of the microscope eyepieces. This azimuth angle was the only datum recorded for each track.

⁴ J. Webb, Eastman Kodak Company, private communication.

The classical expression for the energy of the scattered protons varies as the cosine squared of the proton scattering angle. The incident neutron beam contains the distribution of energies given by Eq. (1), which will be discussed later. This distribution causes the protons that are scattered at any particular angle to also have an energy distribution. The energy distributions for proton recoil angles $\theta_L = 0^\circ, 30^\circ,$ and 45° in the laboratory system are shown in curves *a, b,* and *c* of Fig. 3. Curves of this general form give the emulsion range distributions and also the grain density distributions to be expected of the protons scattered at various angles.

Most spurious tracks were rejected on the basis of having the wrong ionization for their azimuth angle or because they were too short for their angle, although these rejection criteria did not need to be used on more than two percent of the otherwise acceptable tracks. Another reason for the rejection of tracks was that their dive angle into the emulsion was too steep for them to have been caused by protons coming from the beam cylinder. Tracks coming in the three other quadrants were easily eliminated, although their number was very limited. The scanning of vacuum background plates indicated that the confusable background was less than two percent.

Two observers examined 2734 tracks. Of these all proton recoils, 350 in number, observed in the 45° to 51° laboratory angle range were not included in the final results. These tracks were excluded since the specific ionization of tracks scattered at these angles, with energies of 35 to 50 Mev, is so low that an excessive number of tracks is missed by the observer. In addition, 157 tracks in the angular range of 79° to 85° in the laboratory system were not included in the final results since, as will be mentioned later, the correction factor for tracks that do not reach the plates is too large. The two observers read the same plate areas for 200 tracks and found that each missed above five percent of the tracks. The tracks missed were evenly distributed over all angles from 45° to 85° so this is a minor source of error.

The plates used were Ilford, type C-2, with 50-micron emulsions. They were developed for 30 min at 68°F in developer consisting of one part of D19 mixed with six parts of water.

III. TREATMENT OF DATA

The uncorrected data are shown in Fig. 4. The data are grouped into three-degree intervals in the laboratory system, so any corrections in the angular measurement that are small compared to three degrees will not be noticeable. The relativistic correction (Fig. 4, curve *a*) makes the observed laboratory scattering angle slightly smaller than the classical laboratory scattering angle.

The geometry of this experiment, although not nearly so precise as that of Panofsky and Fillmore,³ did not make important corrections necessary. The tracks were observed in swaths 140 microns wide as the slides were

moved under the microscope in a direction parallel to the *x* coordinate (Fig. 2). The swaths were all located, within $\frac{1}{2}$ inch of the edges of the plates nearest the beam. The position of the particular swath, in which the microscope was working within the $\frac{1}{2}$ -in. wide band on the plates, was not recorded as part of the data. It must be pointed out that no attempt was made to determine from which part of the $\frac{1}{2}$ -in. diameter beam cylinder each individual track came, nor was any record kept of the point on the plates at which each particle struck the plates. Thus there is a rectangular distribution of the probability of a particle landing on a plate with a particular value of *y*. In addition the probability of a particle coming from a particular part of the cylindrical, uniform intensity beam is a sine distribution in *z*. These two distributions introduce a geometric uncertainty which must be included in a consideration of the precision of the results. The two probability distributions, one in *y* and one in *z*, must be combined by a folding process, which is really a

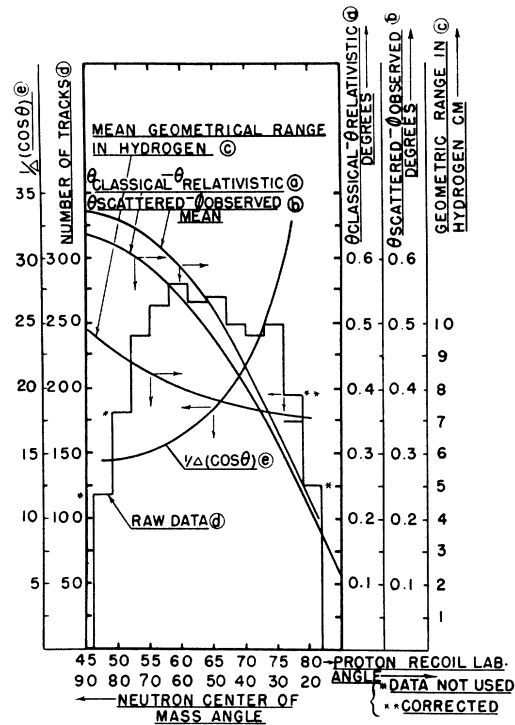


FIG. 4. Functions depending on the laboratory angle at which the protons recoil. Curve (a) gives the difference between the classical recoil angle and the relativistic recoil angle. This correction is seen to be small. Curve (b) shows the mean correction made necessary by the geometry. Curve (c) gives the mean path distance through the hydrogen gas in the scattering chamber from the points of impact in the cylindrical beam region to the photographic plates. Curve (d) is a histogram of the raw data grouped in three-degree intervals. The data from 46° to 52° and from 79° to 82° were considered unreliable for reasons mentioned in the text. The data from 76° to 79° were corrected for limited proton range in the hydrogen and for small angle scattering in the gas and emulsion, as shown. Curve (e) is the multiplication factor for converting the laboratory coordinate data of curve (d) to the center of mass data of Fig. 8. The conversion factor is calculated for the same three-degree intervals into which the data are divided.

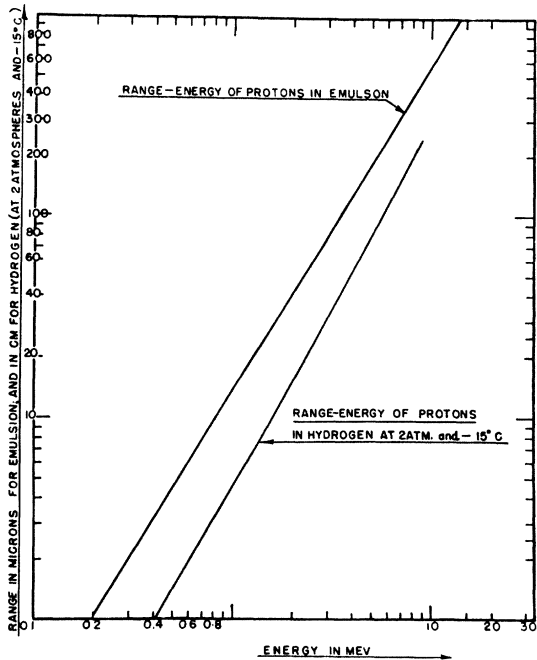


FIG. 5. Range-energy curves for protons in hydrogen gas at 2 atmos and -15°C and in nuclear track emulsion.

two step random walk effect. Due consideration must be given to the geometrical relation between the angle ϕ observed in the microscope and the angle θ_L at which a particular proton is actually scattered from the beam. The mean difference between these two angles shown by curve *b* in Fig. 4 is seen to be less than $\frac{1}{2}^{\circ}$.

The upper limitation on the observable scattering angle θ is introduced by the limited range of the low energy, high angle, protons in the hydrogen gas. The range-energy relations for protons in hydrogen at 2 atmos and -15°C and in nuclear emulsions are shown in Fig. 5. It was decided, on the basis of the experience of Panofsky and Fillmore,³ that emulsion tracks shorter than 30 microns should not be recorded. Tracks shorter than 30 microns are easy to miss in scanning the plates. When tracks shorter than 30 microns are found, it is difficult to make a good measurement of their emulsion entrance angles, and there are also a large number of short background tracks against which it is tedious to discriminate if one tries to measure proton tracks shorter than 30 microns.

Since it was the purpose of this experiment to extend the cross section curve to smaller angles, it is important to investigate the limitations on the acceptability of the data in the range of small neutron scattering angles. There are four effects to be considered in deciding how far into the small angle region the data can be considered dependable. At about $\theta_L = 80^{\circ}$ the energy of the scattered protons becomes so small that all of them do not have a long enough range in the hydrogen gas to allow them to strike the plates. Also, owing to their low energy, they experience appreciable amounts of small

angle scattering in the hydrogen gas and in the photographic emulsions. This scattering introduces errors in the measurements of the scattering angles. Furthermore, in the region of 80° , as a result of the reduced proton energies as mentioned above, the ranges of the particles in the emulsions are in many cases too short to allow for accurate identification and measurement. The combined result of these four effects must be ascertained in order to evaluate the data properly.

The neutron beam produced by the bombardment of a $\frac{1}{2}$ -in. beryllium target with 180-Mev deuterons is known to have a broad energy distribution. This distribution has been calculated by Serber,⁵ and measured by Hadley, *et al.*¹ For energies above the maximum of the distribution curve the calculated and measured results agree, but the measured results are higher than the theoretical ones for energies below the maximum. For the purposes of this experiment it was assumed that the probability $P(E)$ of an incident neutron having the energy E in Mev has the form:

$$P(E) = K \exp\{-[(E-90)/20]^2\}. \quad (1)$$

This relation, (Fig. 3, curve *e*), approximates the high energy distributions of both Serber⁵ and Hadley, *et al.*, but only the measured values of Hadley, *et al.*, for energies less than 90 Mev. It was further assumed that the neutron-proton scattering cross section is inversely proportional to the energy in the energy range considered. Thus the neutron distribution that is effective in producing recoil protons is given by:

$$P'(E)_0 = K(1/E) \exp\{-[(E-90)/20]^2\} \quad (2)$$

(Fig. 3, curve *a*). The integral of this curve gives the fraction of the recoil protons coming from that part of the beam for which the energy is below any given value,

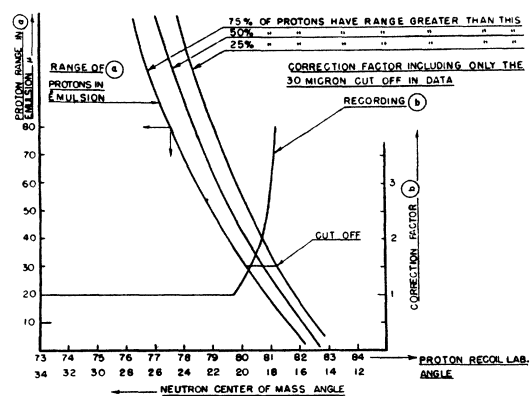


FIG. 6. The experimental cutoff of tracks at the large proton angle limit is based on the three curves (*a*) of proton range in the emulsion for protons scattered at the angles shown, coming from the three positions on the beam energy distribution shown on curve (*d*), Fig. 3. The 30-micron cutoff shown above is explained in the text. Curve (*b*), the multiplicative correction factor that must be applied to the data as a result of the cutoff, is secured from the three curves (*a*) directly, and includes no correction for gas scattering.

⁵ R. Serber, Phys. Rev. **72**, 1007 (1947).

(Fig. 3, curve *d*). This relation will be used to calculate the fraction of the protons with energies too low to reach the plates at large scattering angles where the stopping power of the hydrogen is high. From the range-energy relations for protons, in hydrogen and emulsion (Fig. 5) the energy of the protons entering the emulsion coming from different energy regions of the beam can be calculated as a function of the laboratory proton scattering angle, θ_L . From these energies the ranges in the emulsion for the protons from different beam energy intervals can be plotted as a function of the angle (Fig. 6, curves *a*). Since no tracks shorter than 30 microns are to be considered, there will be a correction factor by which the track counts at various angles ϕ must be multiplied. The cutoff is shown crossing the three beam fraction curves. From the cut-off curve the initial correction curve is calculated (Fig. 6, curve *b*). This correction does not include the effects of gas and emulsion scattering.

In reality the correction factor has a very small influence on the final cross-section curve. The data that go into the single point for neutrons at 26° in the center-of-mass system are 71, 57, and 46 tracks at proton angles, $\theta_L = 76^\circ, 77^\circ,$ and 78° respectively. When the correction factor is applied, the data are changed to 71, 62, and 62, respectively. This application of the cut-off correction factor raises the point at the center-of-mass angle of 26° by about 11 percent.

The corrected track counts, grouped in three-degree intervals, as a function of proton laboratory angle (Table I, column 4) were converted to numbers proportional to the n - p scattering cross section as a function of the neutron center-of-mass angles by the relation:

$$\left(\frac{d\sigma}{d\omega}\right)_{c.o.m.} = \text{const.} N(\phi)_{\Delta\theta} [(z^2 + y^2)/z] (1/\Delta(\cos\theta_{c.o.m.})), \quad (3)$$

where $N(\phi)_{\Delta\theta}$ is the data divided by true scattering angles θ instead of observed angles ϕ . Actually the dif-

TABLE I. Data on the recoil proton tracks.

1	2	3	4	5	6	7
Proton laboratory angle range	No. of tracks observed	Mean neutron cm angle	No. of tracks corrected	$\Delta(\cos\theta)_{cm}$ transformation factor	$\left(\frac{d\sigma}{d\omega}\right)_{cm}$ in 10^{-27} cm ²	Combined probable error
46-48	114	86	114	0.06963		
49-51	181	80	181	0.06874		
52-54	241	74	241	0.06710	4.28	0.19
55-57	260	68	260	0.06472	4.80	0.20
58-60	280	62	280	0.06163	5.42	0.22
61-63	266	56	266	0.05787	5.48	0.22
64-66	270	50	270	0.05347	6.02	0.24
67-69	248	44	248	0.04848	6.11	0.26
70-72	240	38	240	0.04298	6.77	0.29
73-75	248	32	248	0.03699	8.01	0.34
76-78	174	26	195	0.03060	7.60	0.39
79-81	120	20				
82-84	32	14				
Total—2734 tracks observed						

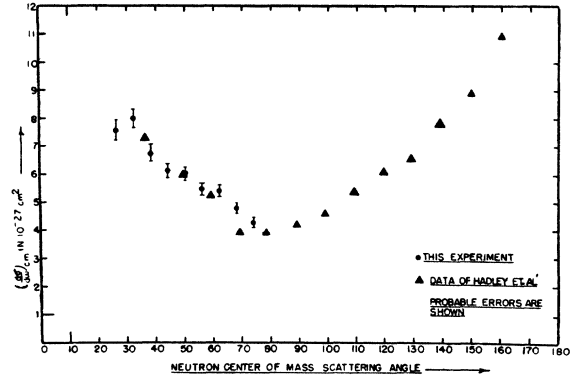


Fig. 7. The final corrected data are shown by the circles above. The results of Hadley, *et al.* (reference 1), are shown by the triangles. It is seen that the slopes of the results of the two experiments agree between 36° and 60° .

ference between these angles (Fig. 4, curve *b*) is such a slowly varying function of the angle that the correction for it was not applied. The geometrical factor $(z^2 + y^2)/z$ is independent of the scattering angle. As a result of the geometrical parameters, when the two $\frac{1}{2}$ -in. geometrical tolerances are combined properly, they produce a probable error of 1.54 in. in the geometrical factor, $(z^2 + y^2)/z$, whose mean value is 13.12 in. This probable error only introduces a very small error into the relative cross section data which is combined with the statistical error and listed in Table I, column 7. The values of the $\Delta(\cos\theta)_{cm}$ factor of Eq. (3) for transformation from laboratory to center-of-mass angles are shown in Table I, column 5. The corrected data divided by these and multiplied by a factor to normalize the results to the absolute cross sections of Hadley *et al.*,¹ are given in Table I, column 6, and plotted with probable errors in Fig. 7, in combination with the points measured by Hadley, *et al.*

IV. CONCLUSIONS

The n - p scattering cross section can be measured with the nuclear emulsion method for 90-Mev neutrons between neutron angles in the center-of-mass system of approximately 26° to 80° . In general the results agree with those secured by Hadley, *et al.*, with counters. The slopes of the curves agree between 36° and 60° . The results of this experiment confirm the increasing slope of the cross-section curve in the small angle region; however, the asymmetry of the curve about 90° is based on the Hadley data since the curve from this experiment is normalized to the Hadley results.

The author wishes to express his appreciation to Keith Brueckner who aided in the design of the apparatus, to Jack Steller who helped with the runs and microscope reading, and to Professor W. K. H. Panofsky, under whose direction the work was carried out.